arXiv:0805.3150v3 [astro-ph] 27 Oct 2008

Galaxy Size Problem at $z = 3$: Simulated Galaxies Are Too Small

M. Ryan Joung[1], Renyue Cen[1], & Greg L. Bryan[2]

ABSTRACT

Using state-of-the-art adaptive mesh refinement cosmological hydrodynamic simulations with a spatial resolution of proper 0.21 h_{73}^{-1} kpc in refined subregions embedded within a comoving cosmological volume $(27.4\ h_{73}^{-1}\,\mathrm{Mpc})^3$, we investigate the sizes of galaxies at $z = 3$ in the standard cold dark matter model where reionization is assumed to complete at $z_{ri} \sim 6$. Our simulated galaxies are found to be significantly smaller than the observed ones: while more than one half of the galaxies observed by HST and VLT ranging from rest-frame UV to optical bands with stellar masses larger than $2 \times 10^{10}\,\mathrm{M}_\odot$ have half-light radii larger than $\sim 2\ h_{73}^{-1}$ kpc, none of the simulated massive galaxies in the same mass range have half-light radii larger than $\sim 2\ h_{73}^{-1}$ kpc, after taking into account dust extinction. Corroborative evidence is provided by the rotation curves of the simulated galaxies with total masses of 10^{11}-$10^{12}\,\mathrm{M}_\odot$, which display values (300-1000 km s^{-1}) at small radii ($\sim 0.5\ h_{73}^{-1}$ kpc) due to high stellar concentration in the central regions, larger than those of any well observed galaxies. Possible physical mechanisms to resolve this serious problem include: (1) an early reionization at $z_{ri} \gg 6$ to suppress gas condensation hence star formation, (2) a strong, internal energetic feedback from stars or central black holes to reduce the overall star formation efficiency, or (3) a substantial small-scale cutoff in the matter power spectrum.

Subject headings: hydrodynamics — galaxies: formation — galaxies: kinematics and dynamics — cosmology: theory — methods: numerical — ultraviolet: galaxies

1. INTRODUCTION

The standard cosmological model has been remarkably successful in accounting for observations on scales larger than galaxy sizes (Krauss & Turner 1995; Ostriker & Steinhardt

[1]Department of Astrophysical Sciences, Princeton University, Peyton Hall, Ivy Lane, Princeton, NJ 08544

[2]Department of Astronomy, Columbia University, Pupin Physics Laboratory, New York, NY 10027

1995; Bahcall et al. 1999; Tegmark et al. 2004; Spergel et al. 2007). We intend to test this same model with regard to galaxy formation and evolution, a regime where astrophysical processes are important and hence a detailed testing of the cosmological model becomes more intricate. In this paper, the first of a series, we focus on the sizes of galaxies at redshift $z = 3$, including "Lyman Break Galaxies" (LBGs) (Steidel et al. 2003). Previous works on this subject include those based on semi-analytic methods (e.g., Mo et al. 1999; Somerville et al. 2001; Somerville et al. 2008); the observed size-mass and size-luminosity relations at $z = 3$ were reproduced in these studies.

Here, we take a brute-force approach using high-resolution adaptive mesh refinement (AMR) cosmological simulations to minimize the number of adjustable astrophysical parameters and thereby maximize the predictability of the standard model. A physical resolution of our simulations of 0.21 h_{73}^{-1} kpc proper at $z = 3$ in refined subregions embedded within a comoving cosmological volume (27.4 h_{73}^{-1} Mpc) permits, an accurate characterization of the sizes of galaxies at $z = 3$. More specifically, we compare the half-light radii of simulated and observed galaxies in terms of size-mass and size-luminosity relations. This comparison is motivated by a series of observations of $z \sim 3$ galaxies in the rest-frame UV (Giavalisco et al. 1996; Lowenthal et al. 1997; Ferguson et al. 2004; Giavalisco et al. 2008) and in the rest-frame optical (Trujillo et al. 2006; Toft et al. 2007; Zirm et al. 2007; Buitrago et al. 2008).

We find the simulated galaxies to be generally smaller than the observed galaxies at $z = 3$ in the stellar mass range $\geq 10^{10.5}\,\mathrm{M}_{\odot}$ where comparisons can be made. This problem may be related to the disk size problem (also called the "angular momentum problem") at $z = 0$ (e.g, Navarro et al. 1995; Navarro & Steinmetz 1997; Governato et al. 2004). The galaxy size problem at $z = 3$ found in the present work may also be related to an apparent large excess of predicted but unobserved dwarf halos (Klypin et al. 1999; Moore et al. 1999) and an over-concentration of dark matter in simulated dwarf galaxies on the scale of $\sim$1 h_{73}^{-1} kpc (Moore 1994; Flores & Primack 1994; Burkert 1995; McGaugh & de Blok 1998; Kravtsov et al. 1998; Moore et al. 1999). Physical processes at high redshift that may be responsible for the eventual resolution of this problem should be manifested more clearly at $z = 3$, as they are unaffected by additional complications that may occur at lower redshifts. Therefore, one may be able to obtain important "cleaner" clues to the nature of the dark matter and/or important astrophysical processes at high redshifts by studying $z = 3$ galaxies. Moreover, combining observations at both $z = 3$ and $z = 0$ may provide still more powerful constraints.

2. SIMULATION AND ANALYSIS METHODS

We perform cosmological simulations with the adaptive mesh refinement (AMR) Eulerian hydro code, Enzo (Bryan 1999; Norman & Bryan 1999; O'Shea et al. 2004). First, we ran a low resolution simulation with a periodic box of 27.4 h_{73}^{-1} Mpc comoving on a side in a ΛCDM universe with cosmological parameters consistent with the WMAP3 results: (Ω_m, Ω_Λ, Ω_b, h, σ_8, n_s) = (0.24, 0.76, 0.042, 0.73, 0.74, 0.95). We identified virialized dark matter halos in this simulation at $z = 3$ and resimulated 11 of the most massive 20 halos in a suite of five high resolution simulations embedded within the same (27.4 h_{73}^{-1} Mpc)^3 comoving box using the multimass initialization technique. The five high resolution subregions have comoving volumes ranging from ∼(3.4 h_{73}^{-1} Mpc)^3 to ∼(8.8 h_{73}^{-1} Mpc)^3. Within the high-resolution regions, the cell size of the root grid is 53.5 h_{73}^{-1} kpc and additional grid refinements are allowed to reach a maximum level of $l_{max} = 6$, resulting in the maximum spatial resolution of 0.84 h_{73}^{-1} kpc (comoving) or 0.21 h_{73}^{-1} kpc (proper) at $z = 3$, while the rest of the box is evolved at a lower resolution of 214 h_{73}^{-1} kpc. The dark matter particle mass in the high-resolution region is 4.6×10^6 $M_\odot$. The simulations include a metagalactic UV background (Haardt & Madau 1996), a diffuse form of photoelectric and photoionization heating (Abbott 1982; Joung & Mac Low 2006) and shielding of UV radiation by neutral hydrogen (Cen et al. 2005). They also include cooling due to molecular hydrogen (Abel et al. 1997) and metallicity-dependent radiative cooling (Cen et al. 1995) extended down to 10 K (Dalgarno & McCray 1972). Star particles are created in cells that satisfy a set of criteria for star formation proposed by Cen & Ostriker (1992). A stellar particle of mass $m_* = c_* m_{\rm gas} \Delta t / t_*$ is created (the same amount is removed from the gas mass in the cell), if the gas in a cell at any time meets the following three conditions simultaneously: (1) contracting flow, (2) cooling time less than dynamic time, and (3) Jeans unstable, where Δt is the time step, $t_* = \max(t_{\rm dyn}, 10^5 {\rm yrs})$, $t_{dyn} = \sqrt{3\pi/(32 G \rho_{tot})}$ is the dynamical time of the cell, $m_{\rm gas}$ is the baryonic gas mass in the cell and $c_* = 0.03$ is star formation efficiency. Each star particle is tagged with its initial mass, creation time, and metallicity; star particles typically have masses of ∼10^5 $M_\odot$. Star formation and supernovae feedback are modeled following Cen et al. (2005) with $e_{SN} = 3 \times 10^{-6}$. Feedback energy and ejected metals are distributed into 27 local gas cells centered at the star particle in question, weighted by the specific volume of each cell. The temporal release of metal-enriched gas and thermal energy at time t has the following form: $f(t, t_i, t_{dyn}) \equiv (1/t_{dyn})[(t - t_i)/t_{dyn}] \exp[-(t - t_i)/t_{dyn}]$, where t_i is the formation time of a given star particle. The metal enrichment inside galaxies and in the intergalatic medium is followed self-consistently in a spatially resolved fashion (Cen et al. 2005).

We identify virialized objects in our high resolution simulations using the HOP algorithm (Eisenstein & Hut 1998), which is tested to be robust. We find 49 halos with virial masses

$> 5 \times 10^{10}$ $M_\odot$ to compare with observations.

The light distribution is computed from the star particles using the GISSEL stellar synthesis code (Bruzual & Charlot 2003). We calculate the luminosities of the simulated galaxies in various rest-frame UV and optical bands where observations are available for $z \sim 3$ galxies with measured half-light radii (see Fig. 2). To obtain half-light radii in the right wavelength range, we placed the same filter (blueshited to z=3) as used in each sample of observed galaxies; this was necessary because the sizes of simulated galaxies vary depending on the observed band, as shown in the size-luminosity plot. We followed the procedure described in Appendix B of Rudnick et al. (2003) to compute luminosities of the model galaxies in each given band.[1] The stellar mass of each simulated galaxy is equal to the sum of the masses of the star particles located within 15% of the virial radius of the galaxy at z=3. For the observed galaxies, we adopt the stellar masses reported in the papers referenced in Figure 2 and, where appropriate, convert apparent magnitudes to luminosities in the wavelength range of the given filter blueshifted to z=3. We adopt an approximate model for dust extinction following Binney & Merrifield (1998) but assume that dust attenuation is proportional to the metal column density rather than the total hydrogen density and correct for depletion of refractory elements (Zn) onto dust grains parametrized by f_{Fe}, fraction of iron in dust (Vladilo & Peroux 2005): $A_V = \Sigma_Z \ f_{Fe}/(4 \times 10^{19} \ m_p F \ \mathrm{cm}^{-2})$ mag, where m_p is the proton mass, Σ_Z is the mass column density of metals in front of a given star particle. The factor, $F = 3.7$, is chosen so that $E(B-V) = 0.3$ (Pettini et al. 1998; Shapley et al. 2003; Steidel et al. 2003), corresponding to $A_{1500\mathring{A}} \approx 1.5$ and an escape fraction in the rest-frame $1500\mathring{A}$ is $\sim$26%. We choose a relatively high value of $E(B-V)$ to strengthen our conclusion that, even though dust extinction acts to increase half-light radii of the galaxies, our simulated galaxies are still generally smaller than the observed ones. The conversions from A_V to A at other bands are based on the dust extinction law proposed by Calzetti et al. (2000). All half-light radii are measured directly using projected 2D maps.

3. RESULTS

Figure 1 shows the projected stellar mass density of a region of comoving size $(1.4 \ h_{73}^{-1} \ \mathrm{Mpc})^2$ with a depth of comoving $3.3 \ h_{73}^{-1}$ Mpc at $z = 3$, cut out from our largest high resolution simulation sub-volume of size $\sim(8.8 \ h_{73}^{-1} \ \mathrm{Mpc})^3$. The insets show magnified images of the four most massive halos in the displayed region in their projected luminosity density distribu-

[1]For photon counting devices, the filter transmission curves $T(\lambda)$ in Rudnick et al. (2003) should be replaced by $T(\lambda)\lambda$.

tions. For each galaxy, the images show, from left to right, intrinsic (before dust attenuation is applied), apparent (after dust attenuation), and smoothed (after dust attenuation and PSF filtering) luminosity densities, respectively, all in the observed I-band.[2] On the one hand, we see that our high resolution permits formation of extremely dense structures. On the other hand, many rich and salient features produced by cosmological processes, such as mergers and tidal tails, are clearly visible and striking. Comparing the leftmost and middle pictures of each row of the insets suggests that dust extinction significantly affects the observed luminosity density distribution in the observed I-band. This can be understood simply as a consequence of the empirical Schmidt-Kennicutt relation (Kennicutt 1998): gas surface density increases monotonically as star formation rate density increases; and we assumed that dust extinction is proportional to the metal surface density hence gas surface density (for a constant metallicity).

Figure 2 shows the size-mass (top) and size-luminosity relations (bottom) of the simulated and observed galaxies. The "intrinsic" half-light radii of the simulated galaxies are displayed as "x", while dust extinction-applied half-light radii are shown as filled circles where the shade in grey scale indicates the amount of dust extinction in the rest-frame V-band (darker for higher extinction; $0.35 \lesssim A_V \lesssim 2.5$). Each sample of observed galaxies is shown by distinct symbols as indicated. The observed $z \sim 3$ galaxies include the rest-frame UV samples from Lowenthal et al. (1997) and Giavalisco et al. (2008) as well as rest-frame optical samples from Trujillo et al. (2006), Toft et al. (2007), Zirm et al. (2007) and Buitrago et al. (2008). In all panels, the intrinsic sizes of the simulated galaxies lie mostly between 0.2 and 0.5 h_{73}^{-1} kpc, while the dust extinction-applied sizes can be significantly larger. This increase in apparent sizes is, on average, greater at shorter wavelengths and for more massive and luminous galaxies, and may be partly responsible for the observed relation between star formation and size at $z \sim 2.5$ (Toft et al. 2007; Zirm et al. 2007). Remarkably, this trend is also seen in the sizes of the simulated galaxies measured in the rest-frame optical bands.

In the top display of Figure 2, the observational data are only available for galaxies with stellar masses of $\geq 2 \times 10^{10}\,\mathrm{M}_\odot$. In this mass range, there are more than one half of the observed galaxies having the half-light radii (all measured in the rest-frame optical) greater than 2 h_{73}^{-1} kpc, whereas all of the simulated galaxies in the same mass range have the half-light radii smaller than 2 h_{73}^{-1} kpc. A significant fraction of these relatively massive galaxies that are actively star-forming (SFR $> 10\,\mathrm{M}_\odot\,\mathrm{yr}^{-1}$) may be identified with the LBGs (Steidel et al. 1996).

This discrepancy in half-light radii between simulated and observed galaxies is also

[2]We use the response curve for the F814W filter on HST's WFPC2.

seen in the size-luminosity relation at the bottom display of Figure 2, where luminosities at several different observed bands are shown in four separate panels. Here, the half-light radii of the simulated galaxies again occupy the low-end of the distributions compared to galaxies observed in the HST WFPC2 F814W filter (Lowenthal et al. 1997), in the VLT ISAAC K_s band (Trujillo et al. 2006; Toft et al. 2007). However, the situation here is slightly more complicated in that we find apparent agreement between simulated galaxies and observations of Giavalisco et al. (2008) in the HST ACS F850LP filter and, to some degree, of Buitrago et al. (2008) in the VLT ISAAC K_s band. Whether the discrepancy among observed sizes is real or an artifact of the different source extraction and fitting algorithms employed is an open question.[3]

Overall, we conclude that there is fairly strong indication that the simulated massive galaxies are too small compared to their observed counterparts at $z \sim 3$, from rest-frame UV to rest-frame optical bands. This suggests that the concurrent star formation activities and the overall stellar mass distributions in the simulated galaxies at $z = 3$ are both too concentrated near the galactic centers. Concentration of stellar mass may be shown in an alternative way using rotation curves. Figure 3 shows rotation velocity curves for the three top galaxies of total mass of $10^{11} - 10^{12}\,M_\odot$. These curves seem to peak at too high a value (300-1000 km s^{-1}) at small radii ($\sim$0.5 h_{73}^{-1} kpc).

It is prudent to ask if our results depend on limited resolution. To address this point, we ran higher resolution simulations (with the smallest cell size of 0.11 proper h_{73}^{-1} kpc or twice the linear resolution as in our fiducial models) of 2 of the 5 subvolumes, or 8 of the 49 galaxies discussed in this Letter. In all of these cases, we find that both the intrinsic half-mass and intrinsic half-light radii are significantly smaller (by nearly a factor of 2), indicating that our results have not yet converged in terms of obtaining the absolute sizes of the high-z galaxies. We find that the dust attenuated half-light radii with the higher resolution simulations are slightly smaller (10-30%) than those from lower resolution simulation. While the absolute sizes have not converged, these tests support and strengthen our conclusion that the simulated galaxies at $z = 3$ are too small compared to their observed counterparts.

[3]We note, however, that the measured half-light radii in Giavalisco et al. (2008) – based on the SExtractor program – may be biased low compared to size measurements derived from fits to Sersic profiles, for the faint galaxies in their sample (M. Giavalisco, private comm.).

4. DISCUSSION AND CONCLUSIONS

The standard cold dark matter cosmological model is in good agreement with a rich set of observations on large scales. Our main purpose is to systematically examine it, through a series of papers, in the context of galaxy formation and evolution, a regime where, relatively speaking, it has not been seriously contested. Because astrophysical processes tend to play a progressively more important role at smaller scales, in particular, on galactic scales and smaller, it is vital to employ as few adjustable astrophysical parameters as possible, to have a true test of the cosmological model.

In this paper we focus on the sizes of galaxies, including LBGs (Steidel et al. 2003) at redshift $z = 3$, using state-of-the-art AMR cosmological hydrodynamic simulations with a spatial resolution of proper 0.21 h_{73}^{-1} kpc in five refined subregions embedded within a comoving cosmological volume $(27.4\ h_{73}^{-1}\,\mathrm{Mpc})^3$. We find that, taking into account dust extinction, the computed distribution of half-light radii of simulated galaxies in the rest-frame I- and V-bands occupy only the low-end of the observed size distributions. While none of the simulated massive galaxies have half-light radii larger than $\sim$2 h_{73}^{-1} kpc, more than one half of the observed galaxies have half-light radii exceeding that value. We note that the intrinsic (i.e., in the absence of dust extinction and finite instrumental resolution) half-light (and half-stellar-mass) radii are smaller at $\sim 0.3\ h_{73}^{-1}$ kpc and our resolution tests indicate that they become still smaller with higher resolution, hence strengthening our conclusions. Consistent with this apparent discrepancy between simulated and observed LBGs, the rotation curves of the simulated galaxies of total masses of 10^{11}-$10^{12}\,\mathrm{M}_\odot$ have unusually high values (300-1000 km s^{-1}) at small radii ($\sim$0.5 h_{73}^{-1} kpc). Such rotation curves are not seen in local galaxies for which accurate measurements are available, although no direct comparison with observed high-redshift galaxies can be properly made at this time.

These discrepancies appear to originate from stellar masses that are too highly concentrated in small ($< 1\ h_{73}^{-1}$ kpc) central regions of the simulated galaxies. This may be caused by an over-abundance of smaller galaxies that formed at high redshifts and subsequently sank to the centers via dynamical friction *or* by vigorous *in situ* star formation in the central regions. Likely, any potential viable solution to this apparent problem would have to reduce the amount of stars that formed. Possible physical mechanisms include: (1) an early reionization with $z_{ri} \gg 6$ to suppress gas condensation that will reduce earlier star formation (e.g., Bullock, Kravtsov, & Weinberg 2000), (2) a strong, internal energetic feedback from stars or central black holes to reduce the overall star formation efficiency (e.g., Sommer-Larson et al. 2003; Governato et al. 2007), or (3) a substantial small-scale cutoff in the matter power spectrum, for example, if the dark matter particles are warm rather than cold (e.g., Hogan & Dalcanton 2000; Sommer-Larsen & Dolgov 2001; Bode, Ostriker & Turok 2001)

Since the age of the universe at $z = 3$ is only about 1/6 of the present age, a successful resolution to the galaxy size problem at $z \sim 3$ may provide important "cleaner" clues to the nature of the dark matter and/or important astrophysical processes at high redshifts. Moreover, combining observations at both $z = 3$ and $z = 0$ may provide still more powerful constraints.

We thank A. Burkert, Y.-T. Lin, M.-M. Mac Low, L. Mayer, B. Moore, R. Overzier, A. Shapley, and P. van Dokkum for helpful discussions and comments; F. Buitrago, M. Giavalisco, M. Kriek, G. Rudnick, and I. Trujillo for generous help with observational data; and M.-S. Shin and K. Nagamine for help with the galaxy spectrum code. We are grateful to M. Giavalisco and his colleagues for making their new GOODS-S sample available to us prior to publication. We are indebted to an anonymous referee for many useful suggestions that help improve the paper. We thank M. Norman and his team in University of California at San Diego for useful assistance in code development. We gratefully acknowledge financial support by grants AST-0507521, NNG05GK10G and NNX08AH31G. The simulations were performed at NCSA with computing time provided by LRAC allocation TG-MCA04N012.

REFERENCES

Abbott, D. C. 1982, ApJ, 263, 723

Abel, T., Anninos, P., Zhang, Y., & Norman, M. L. 1997, New Astronomy, 2, 181

Bahcall, N.A., Ostriker, J.P., Perlmutter, S., & Steinhardt, P. 1999, Science, 284, 1481

Binney, J., & Merrifield, M. 1998, Galactic Astronomy (Princeton: Princeton Univ. Press)

Bode, P., Ostriker, J.P., & Turok, N. 2001, ApJ, 556, 93

Bruzual, G., & Charlot, S. 2003, MNRAS, 344, 1000

Bryan, G. L., 1999, Comp. Sci. Eng., 1, 46

Buitrago, F., Trujillo, I., Conselice, C. et al., 2008, ApJL, in press (arXiv:0807.4141v2 [astro-ph])

Bullock, J.S., Kravtsov, A.V., & Weinberg, D.H. 2000, 539, 517

Burkert, A. 1995, ApJ, 447, L25

Calzetti, D., Armus, L., Bohlin, R. C. et al. 2000, ApJ, 533, 682

Cen, R., & Ostriker, J.P. 1992, ApJ, 399, L113

Cen, R., Kang, H., Ostriker, J.P., & Ryu, D. 1995, ApJ, 451, 436

Cen, R., Nagamine, K., & Ostriker, J.P. 2005, ApJ, 635, 86

Dalgarno, A., & McCray, R.A. 1972, ARA&A, 10, 375

Eisenstein, D.J., & Hut, P. 1998, ApJ, 498, 137

Ferguson, H., Dickinson, M., Giavalisco, M. et al. 2004, ApJ, 600, L107

Flores, R.A., & Primack, J.R. 1995, ApJ, 457, L5

Giavalisco, M., Steidel, C.C., & Macchetto, F.D. 2004, ApJ, 607, 688

Giavalisco, M. and the GOODS Team, 2008, in preparation

Governato, F., et al. 2004, ApJ, 607, 688

Governato, F., et al. 2007, MNRAS, 374, 1479

Haardt, F., & Madau, P. 1996, ApJ, 461, 20

Hogan, C.J., & Dalcanton, J.J. 2000, PhRvD, 62, 063511

Joung, M.K.R., & Mac Low, M.-M. 2006, ApJ, 653, 1266

Kennicutt, R.C., Jr. 1998, ARA&A, 36, 189

Klypin, A.A., Kravtsov, A.V., Valenzuela, O., & Prada, F. 1999, ApJ, 522, 82

Krauss, L., & Turner, M.S. 1995, Gen. Rel. Grav., 27, 1137

Kravtsov, A.V., Klypin, A.A., Bullock, J.S., & Primack, J.R. 1998, ApJ, 502, 48

Lowenthal, J.D., Koo, D.C., Guzman, R. et al. 1997, ApJ, 481, 673

McGaugh, S.S., de Blok, W.J.G. 1998, ApJ, 499, 41

Mo, H.J., Mao, S., & White, S.D.M. 1999, MNRAS, 304, 175

Moore, B. 1994, Nature, 370, 629

Moore, B., Quinn, T., Governato, F. et al. 1999, MNRAS, 310, 1147

Navarro, J.F., Frenk, C.S., & White, S.D.M. 1995, MNRAS, 275, 56

Navarro, J.F., & Steinmetz, M. 1997, ApJ, 478, 13

Norman, M. L., & Bryan, G. L. 1999, ASSL Vol. 240: Numerical Astrophysics, 19

O'Shea, B. W., Bryan, G. L., Bordner, J., Norman, M. L. et al. 2004, "Adaptive Mesh Refinement - Theory and Applications", ed. T. Plewa, T. Linde & V. G. Weirs, Springer Lecture Notes in Comp. Sci. Eng. (arXiv:astro-ph/0403044)

Ostriker, J.P., & Steinhardt, P. 1995, Nature, 377, 600

Pettini, M., Kellogg, M., Steidel, C.C., Dickinson, M., Adelberger, K.L., & Giavalisco, M. 1998, ApJ, 508, 539

Rudnick, G., Rix, H.-W., Franx, M. et al. 2003, ApJ, 599, 847

Shapley, A.E., Steidel, C.C., Pettini, M., & Adelberger, K.L. 2003, ApJ, 588, 65

Somerville, R.S., Primack, J.R., & Faber, S.M. 2001, MNRAS, 320, 504

Somerville, R.S., Barden, M., Rix, H.-W. et al. 2008, ApJ, 672, 776

Sommer-Larsen, J., & Dolgov, A. 2001, ApJ, 551, 608

Sommer-Larsen, J., Gotz, M., & Portinari, L. 2003, ApJ, 596, 47

Spergel, D.N., et al. 2007, ApJS, 170, 377

Steidel, C.C., Giavalisco, M., Pettini, M. et al. 1996, ApJ, 462, 17

Steidel, C.C., Adelberger, K.L., Shapley, A.E. et al. 2003, ApJ, 592, 728

Tegmark, M., et al. 2004, Phys. Rev. D69, 103501

Toft, S., van Dokkum, P., Franx, M. et al. 2007, ApJ, 671, 285

Trujillo, I., Förster Schreiber, N.M., Rudnick, G. et al. 2006, ApJ, 650, 18

Vladilo, G., Peroux, C., 2005, A&A, 444, 461

Zirm, A.W., van der Wel, A., Franx, M. et al. 2007, ApJ, 656, 66

This preprint was prepared with the AAS LaTeX macros v5.2.

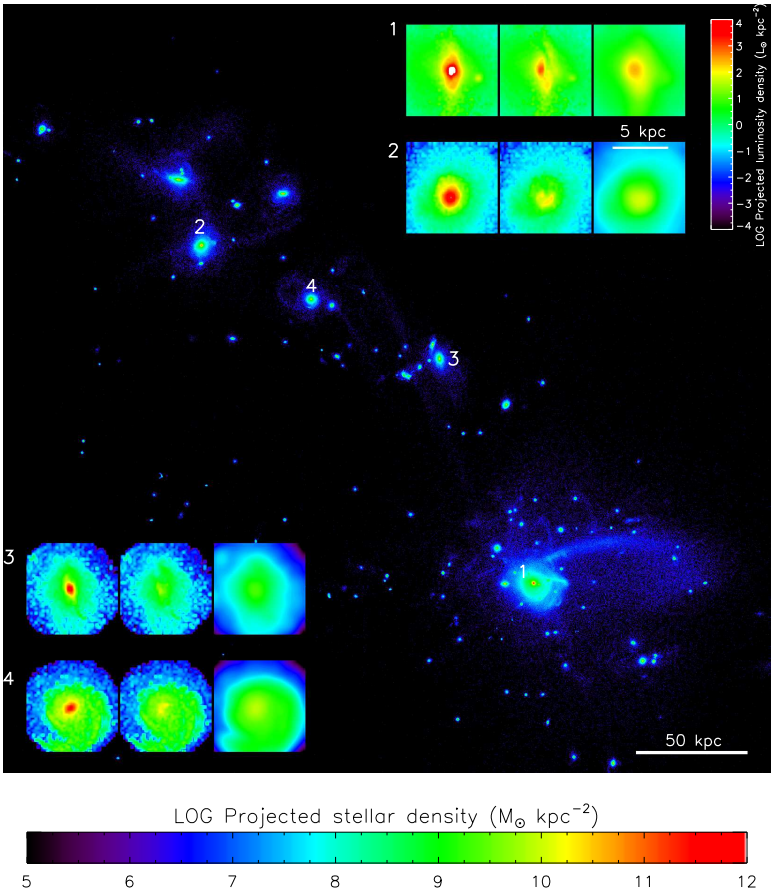


Fig. 1.— The large image displays the projected stellar mass density of a region of comoving size $(1.4\ h_{73}^{-1}\ \mathrm{Mpc})^2$ with a depth of comoving $3.3\ h_{73}^{-1}\ \mathrm{Mpc}$ at $z = 3$, cut out from one of our simulation volumes. The insets zoom in on the four most massive galaxies in volume region in terms of virial mass and show their projected luminosity density distributions. For each galaxy, the images show, from left to right, intrinsic (before dust attenuation is applied), apparent (after dust attenuation), and smoothed (after dust attenuation and PSF filtering) luminosity densities, respectively, all in the observed I-band. A Gaussian filter with FWHM $= 0''.125$ is applied for the PSF. The bars indicate lengths in proper $h_{73}^{-1}\ \mathrm{kpc}$.

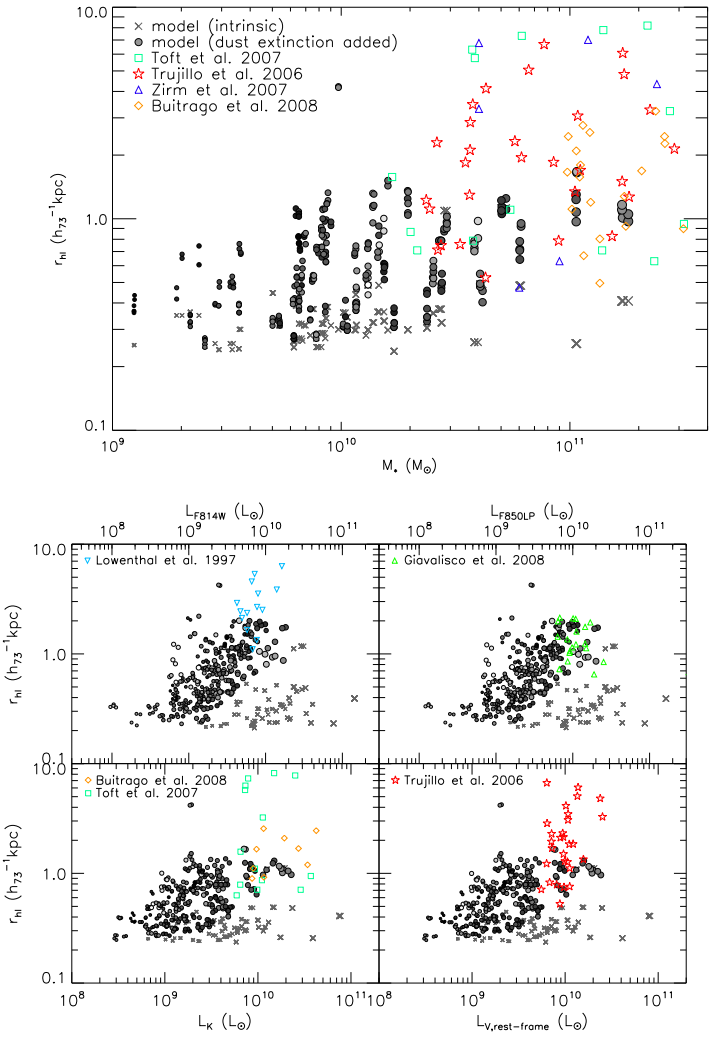


Fig. 2.— Size-mass (*top*) and size-luminosity (*bottom*) relations of the simulated and observed galaxies. The "intrinsic" half-light radii of the simulate galaxies (along six orthogonal projection directions) are displayed as crosses, while dust extinction-applied half-light radii are shown as filled circles where the shade in grey scale indicates the amount of dust extinction in the rest-frame V-band (darker for higher extinction; $0.35 \lesssim A_V \lesssim 2.5$). In the top display the observed galaxies that appear in the size-mass relation are based on measurements in the rest-frame optical. In the bottom display the size-luminosity relations are shown for both rest-frame UV (*top panels*) and rest-frame optical (*bottom panels*). The observed $z \sim 3$ galaxies include the rest-frame UV samples from Lowenthal et al. (1997) using HST WFPC2 F814W filter ($\lambda_c = 8203\mathring{A}$ and FWHM=$1758\mathring{A}$) and from Giavalisco et al. (2008) using HST ACS F850LP filter ($\lambda_c = 8950\mathring{A}$ and FWHM=$900\mathring{A}$), rest-frame optical samples from Trujillo et al. (2006), Toft et al. (2007) and Buitrago et al. (2008) using VLT ISAAC K_s band ($\lambda_c = 21600\mathring{A}$ and FWHM=$2700\mathring{A}$) and from Zirm et al. (2007) using HST WFPC2 F160W filter ($\lambda_c = 16089\mathring{A}$ and FWHM=$4010\mathring{A}$).

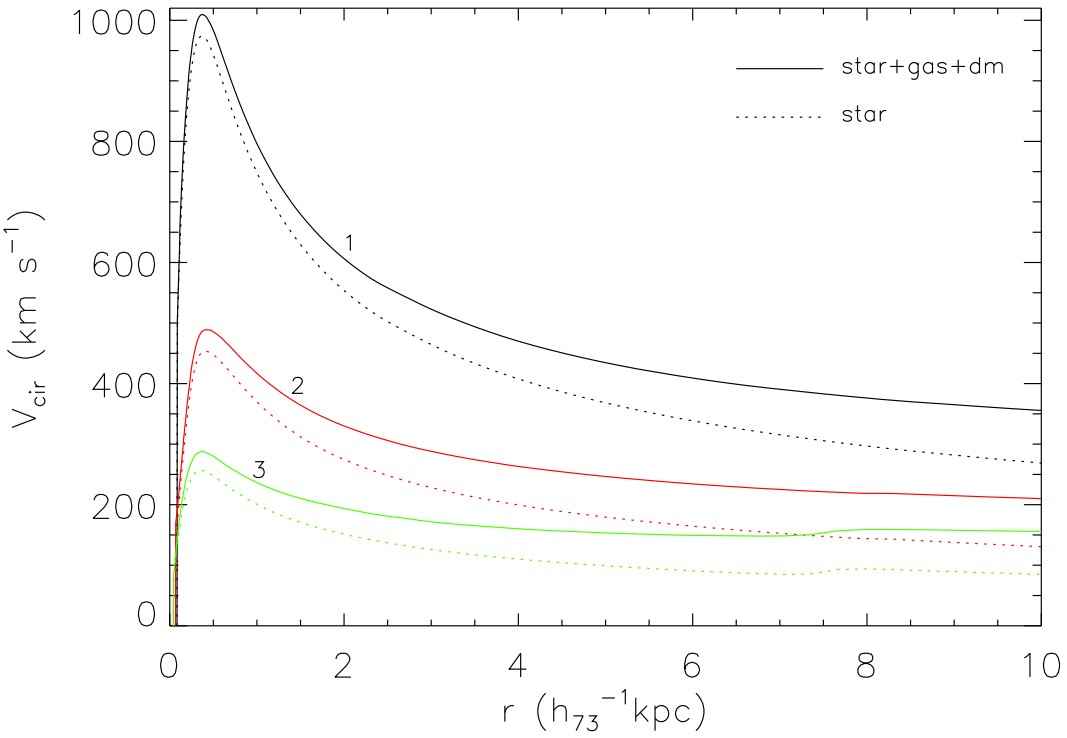


Fig. 3.— Rotation velocity curves for the three galaxies labeled "1", "2" and "3" in Fig. 1. The solid curves represent rotation velocities due to all the matter within a given galactocentric radius, while the dotted curves show those due to stellar mass only. The virial masses of the three galaxies are 8×10^{11}, 4×10^{11} and $1 \times 10^{11}\,M_{\odot}$, respectively.